

Online Supplemental Material

Video 1. *Transient interaction between mRFP-Atg9 and GFP-DFCP1*

HEK293 cells expressing GFP-DFCP1 (green) and mRFP-Atg9 (red) were shifted to starvation medium 5 min before imaging. Cells were imaged at 37°C by time-lapse widefield microscopy using a Nikon Eclipse TE2000-E microscope and a 60x objective. Frames were taken every 5s for 10min. Selected frames (one every other) are shown in Figure 2C'.

Video 2. *Transient interaction between mRFP-Atg9 and GFP-LC3*

HEK293 cells stably expressing GFP-LC3 (green) and mRFP-Atg9 (red) were shifted to starvation medium 5 min before imaging. Cells were imaged at 37°C by time-lapse widefield microscopy using a Nikon Eclipse TE2000-E microscope and a 60x objective. Frames were taken every 5s for 10min. Selected frames (every other one) are shown in Figure 2D'.

Supplementary Figure legends

Figure S1. Autophagy is impaired in Atg9KO MEFs. (A) MEFs from wt and Atg9^{-/-} mice were incubated in full (F) or starvation medium (S) for 2 h. Cell lysates were resolved by SDS-PAGE and analyzed by western blotting for mAtg9, actin and LC3. (B) LC3-II ratio normalized to actin or LC3-I from 3 experiments as in A. Error bars, SEM; two-tailed unpaired t test. (C) Confocal microscopy of wild type and Atg9^{-/-} MEFs, incubated in starvation medium for 2 h before fixation. LC3 (green) and WIPI2 (red) were detected using indirect immunofluorescence. (D) Quantification of LC3-positive structures in WT versus Atg9 KO MEFS and (E) Quantification of spot diameter in WT versus Atg9 KO MEFS.

Figure S2. Characterisation of HEK293/mRFP-Atg9 stable cell lines. (A) Confocal microscopy of HEK293/mRFP-Atg9 incubated in full or starvation medium for 2 h. TGN46 (green) was detected by indirect immunofluorescence. As expected, mRFP-Atg9 colocalizes with TGN46 and disperses upon starvation. (B) HEK293, HEK293/mRFP-Atg9 (clone 1F10), HEK293/GFP-LC3 (clone 2GL9), HEK 293/GFP-LC3/mRFP-Atg9 (clone 9B9) were incubated in full (F) or starvation medium (S) for 2 h with or without (+/-) the vacuolar-type H⁺ ATPase inhibitor Bafilomycin A1. Cell lysates were resolved by SDS-PAGE and analyzed by western blot using antibodies against mAtg9, β -tubulin and LC3. (C) Quantification of LC3-I and LC3-II for the clones shown in B expressed as LC3-I/LC3-II ratio (n=2). Note that starvation-dependent induction and lysosomal turnover are indistinguishable between the cell line expressing mRFP-Atg9 and the parental cell line (compare 1F10 with wt HEK293 and 9B9 with 2GL9). Western blots are taken from the same experiment, at the same exposure, but from different gels, thus are not directly comparable.

Figure S3. CLEM and cryo-immuno-EM of mAtg9. (A) Confocal microscopy and low magnification TEM (Ai, Aii) of HEK293/GFP-LC3/mRFP-Atg9 cell shown in Figure 4A. The boxed region in A corresponds to inset in Figure 4A. The boxed

region in Ai corresponds to Aii while the boxed region in Aii corresponds to the area shown in Figure 4B and C. Ai, bar 10 μ m; Aii, bar 2 μ L. (B-E) Cryo-immuno-EM of starved HEK293/GFP-LC3/mRFP-Atg9 labelled for mAtg9. mAtg9 is found on vesicles and tubules surrounding an endosome (B and E) or scattered in the cytosol (C and D). m, mitochondria, e, endosome, a, autolysosome, g, golgi. C, F: bar, 500nm; D, E: bar 200nm.

Figure S4. Identification of endosomal mAtg9 interactors. (A) Lysates from HEK293 cells transfected with an empty vector (-) or HA-mAtg9 (+) were immunoprecipitated with a mouse anti-HA antibody. Tot, 3% of total lysate; U, 3% of unbound after IP; IP: immunoprecipitation lanes. HA-mAtg9-Gly represents normally glycosylated HA-mAtg9. Overexpression of mAtg9 can result in some unglycosylated protein (HA-mAtg9), which is not indicative of an ER localization (data not shown). (B) Colloidal coomassie staining of gel, prior to Mass Spectrometry analysis. HEK293 cells that were mock transfected or expressing HA-mAtg9 were incubated in full medium (F) or starved for 2 h (S) before lysis and immunoprecipitation as in A. The entire lane was cut into 48 bands and subjected to analysis. (C) Selected list of putative Atg9 interactors that were found by mass spectroscopy (n=2). Each experiment was performed in fed and starved conditions and the number of peptides recovered in each condition is indicated. No peptides for these interactors were detected in mock transfected samples. (D) HEK293 cells mock transfected (-) or expressing HA-mAtg9 (+) were incubated in full medium (F) or starved for 2 h (S) before lysis and immunoprecipitation with anti-HA antibody followed by western blotting for TfR and CI-MPR. (E) HEK293 cells were lysed and Atg9 was immunoprecipitated in Chaps buffer. Input (Inp), unbound and bound proteins were blotted for Atg9, TnR and Syntaxin13, a RE SNARE protein. Note Syntaxin13 does not co-immunoprecipitate indicating the specificity of the Atg9-TfR interaction.

Figure S5. mAtg9 dispersion and autophagy do not require retromer. (A) Confocal microscopy of HEK293 cells treated with siRNAs against RISC-Free (ctrl) or Vps26. Vps26 (green) and mAtg9 (red) were detected by indirect immunofluorescence and the inset shows partial colocalization between the two. Only cells depleted of Vps26, as indicated by the asterisk, were considered for the analyses in B and C. (B) HEK293 cells, either control (ctrl) or treated with siRNA against Vps26, were either incubated

for 2 h in full medium (Fed), starved for 2 h (Stv) or starved for 2 h and then allowed to recover for 30min in full medium in the presence of the protein synthesis inhibitor cycloheximide (Rec). Cells were then fixed and endogenous mAtg9 was detected by indirect immunofluorescence. (C) Cells from (B) having a dispersed mAtg9 distribution were blinded and counted manually and expressed as percent of total (n=2). White bars, ctrl; Grey bars, Vps26 knock down. (D) Western blot analysis of cell lysates from control and Vps26-depleted cells. Residual levels of Vps26 after siRNA depletion ranged between 10 and 20% of control. (E) Neither LC3 lipidation, nor turnover of LC3-II is inhibited in Vps26 knocked down cells as revealed by quantification of LC3-II/LC3-I ratio in (D). F, full medium; S, starvation; R, 2 h starvation + 30 min recovery (n=2).

Figure S6. Ficoll Gradient Analysis. (A) LC3-II/LC3-I ratio from two experiments as in Figure 7. Both WIPI2 and ULK1 knockdown substantially reduce LC3 lipidation. (B) The refractive index of each fraction was determined and plotted against the fraction number. One representative experiment out of 2 is shown. In the interval between fraction 6 and 24, the 4 gradients are linear and comparable within each other. (C) To allow comparison between experiments, mAtg9 profiles from 4 fractionation experiments (as in Figure 8) were plotted against the refractive index of each fraction (solid line) and fitted to a Gaussian curve (dashed line). The profiles of mAtg9 in fed (black) or starved (red) conditions from 4 experiments are shown.

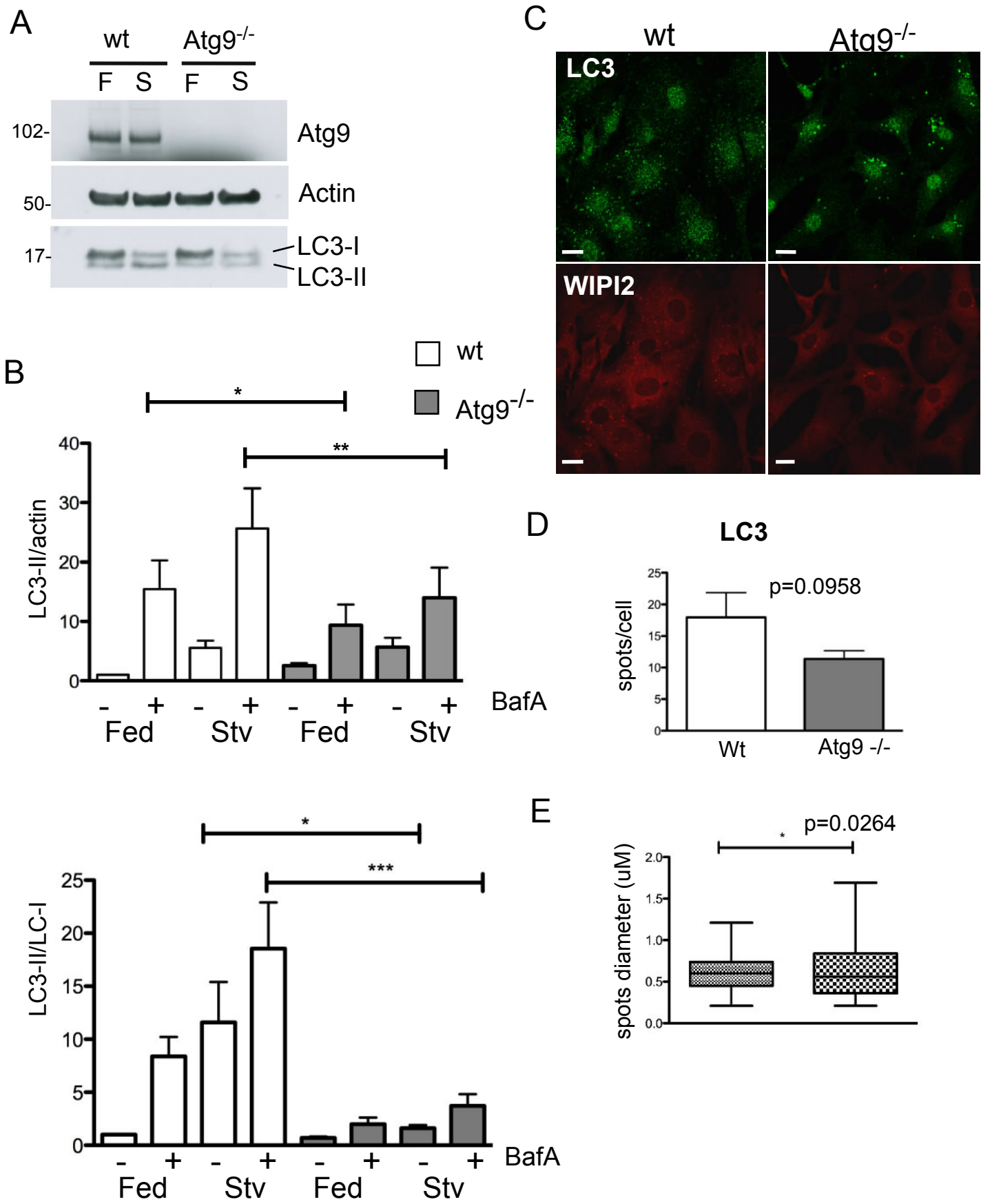


Fig. S1

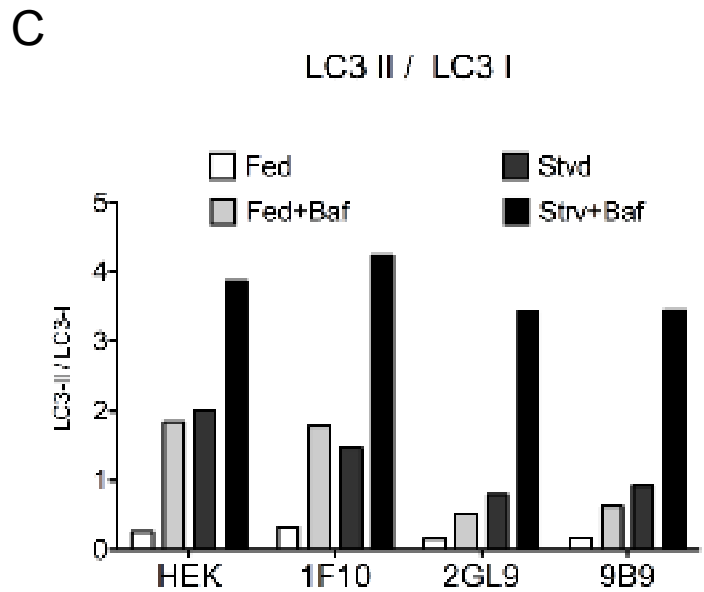
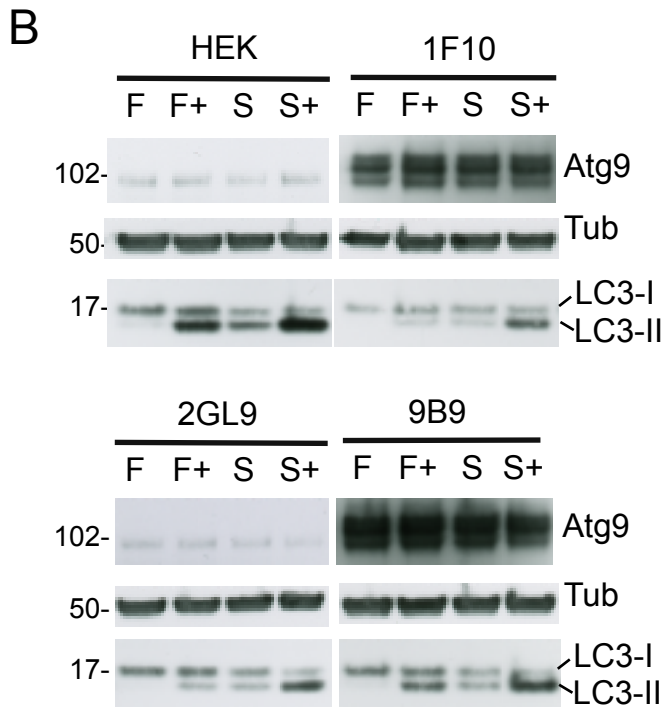
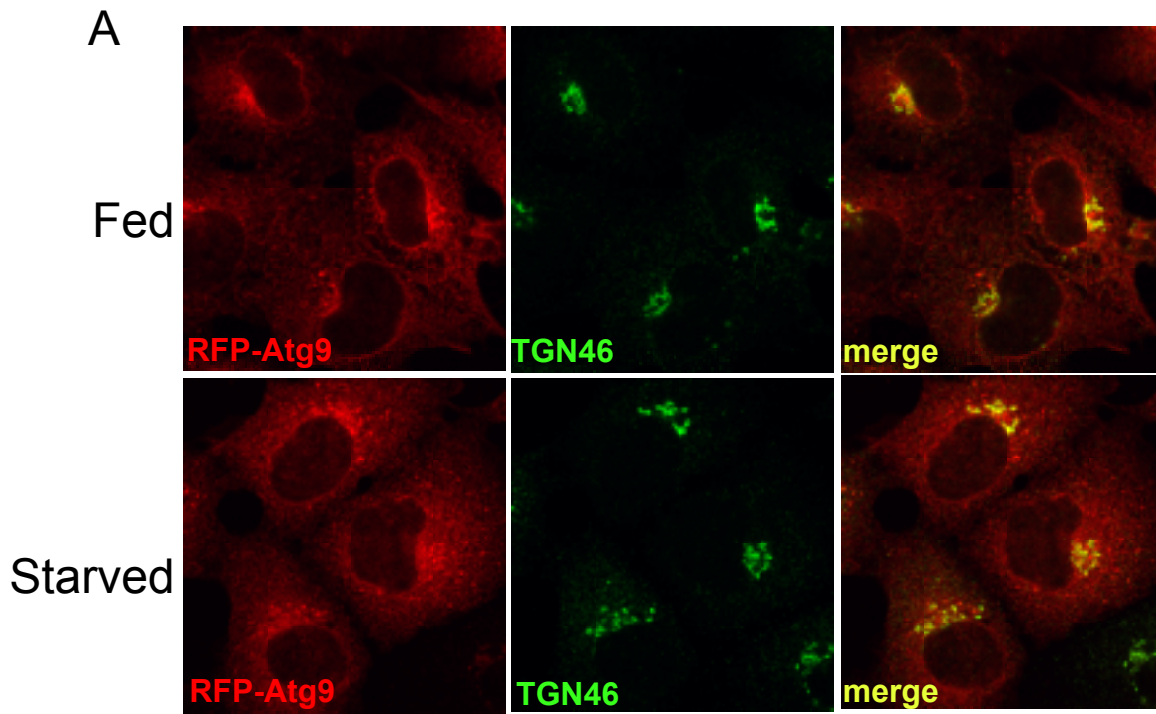


Fig. S2

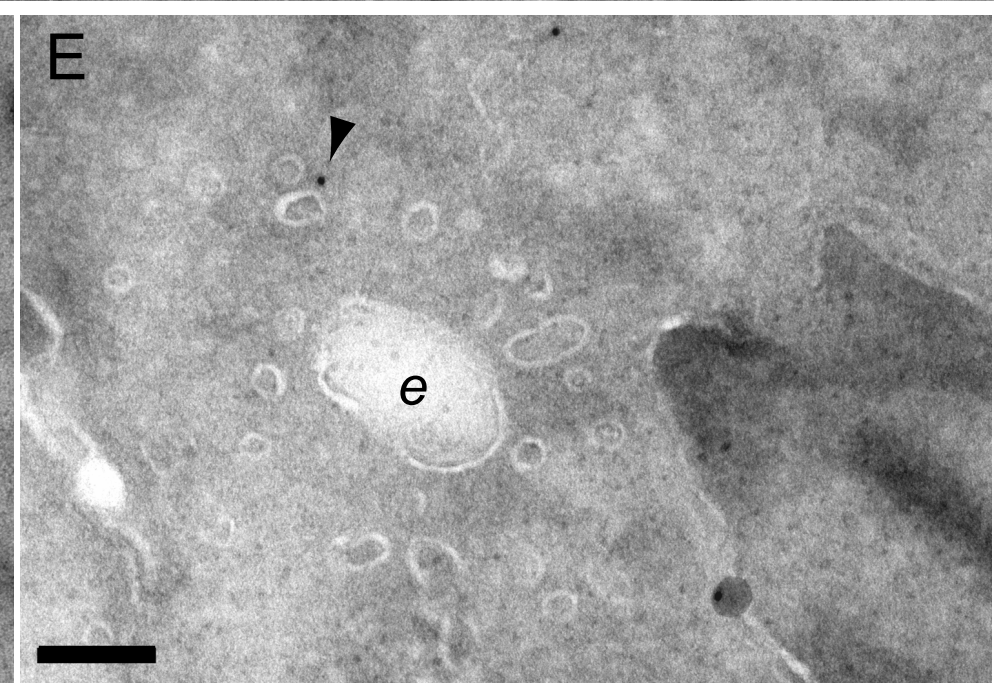
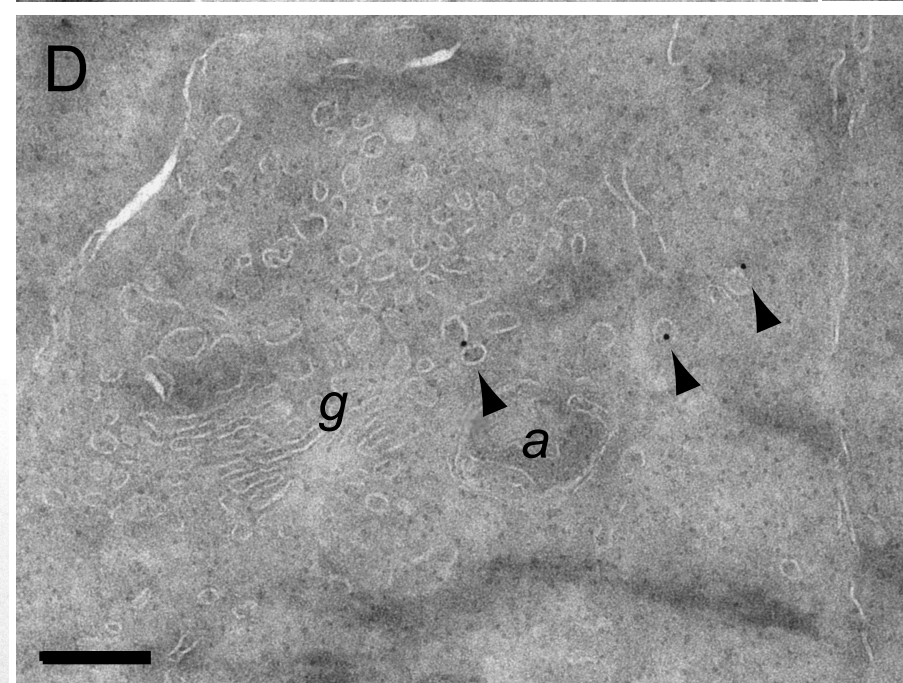
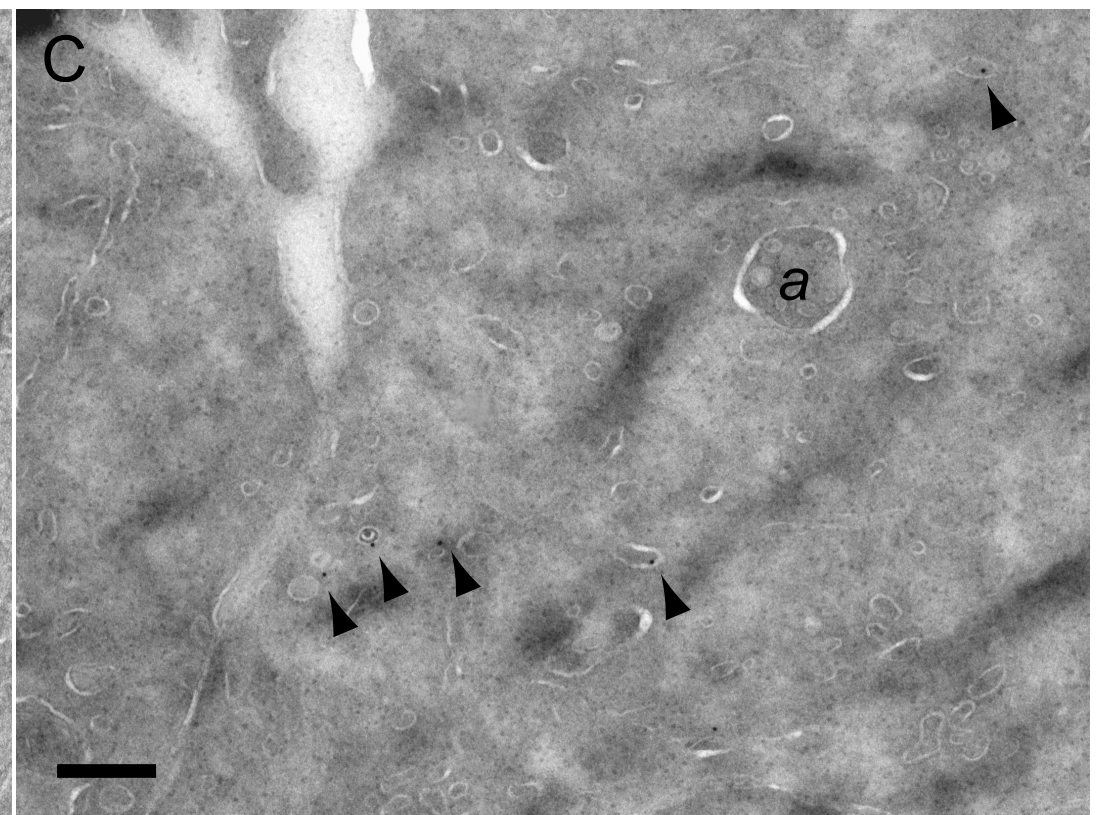
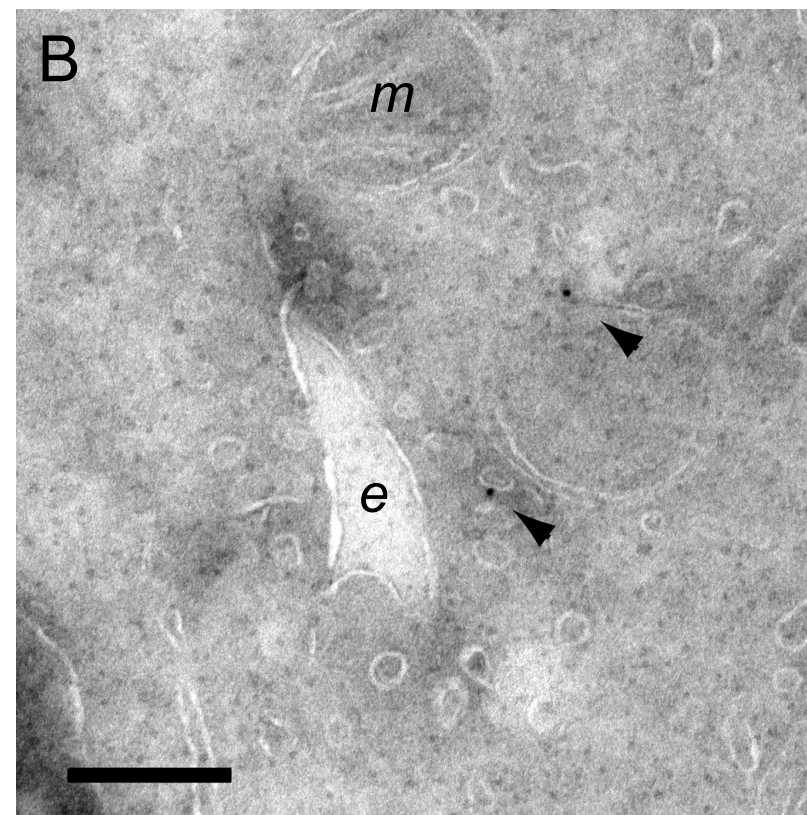
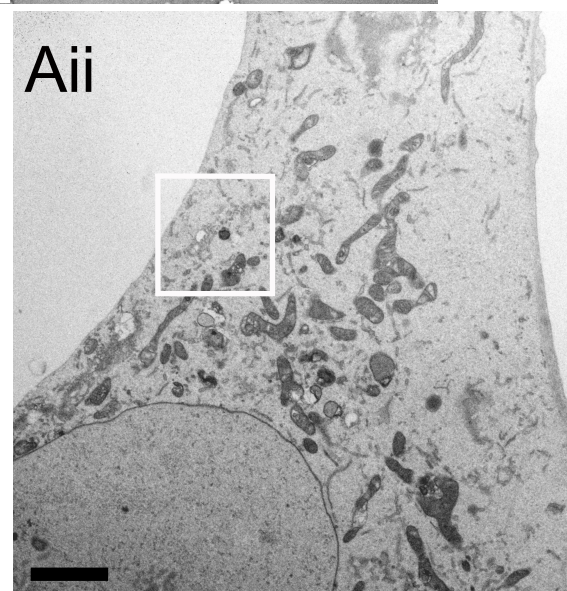
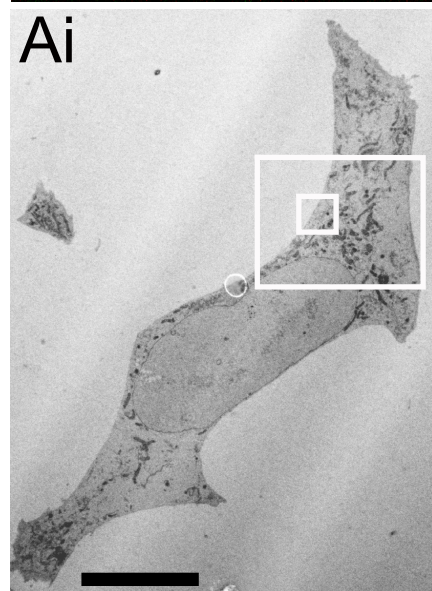
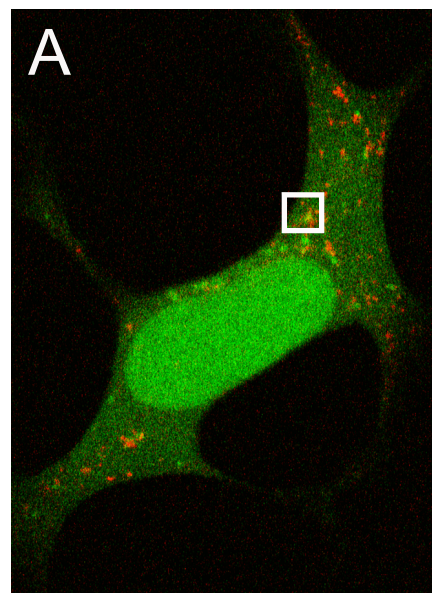
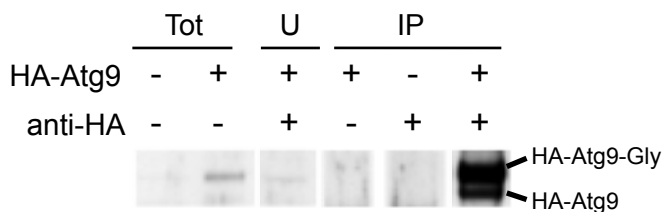
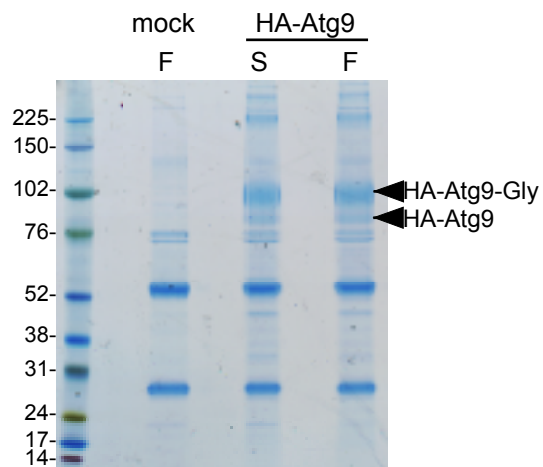


Fig. S3

A



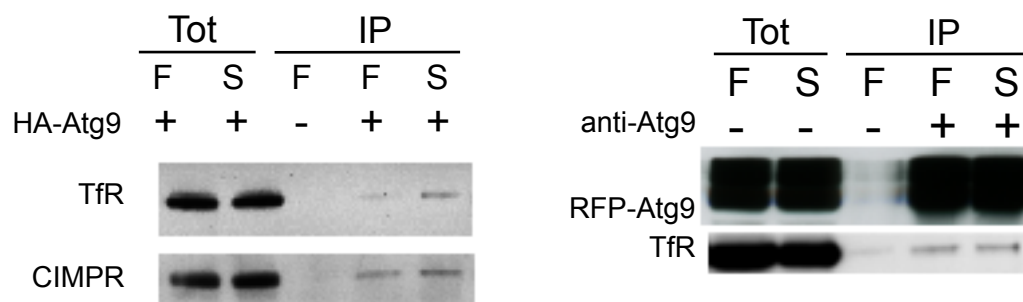
B



C

Protein name	Accession no.	fed#1	stvd#1	fed#2	stvd#2
Cation-independent mannose-6-phosphate receptor	P11717	1	2	12	11
Transferrin receptor protein 1	P02786	3	8	10	11

D



E

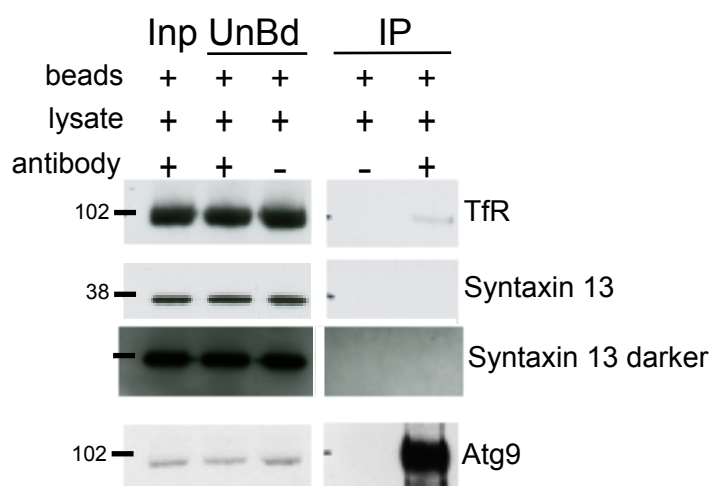


Fig. S4

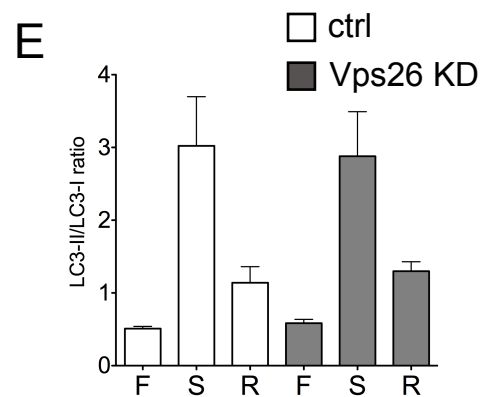
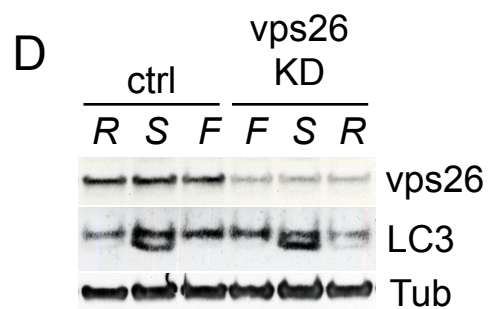
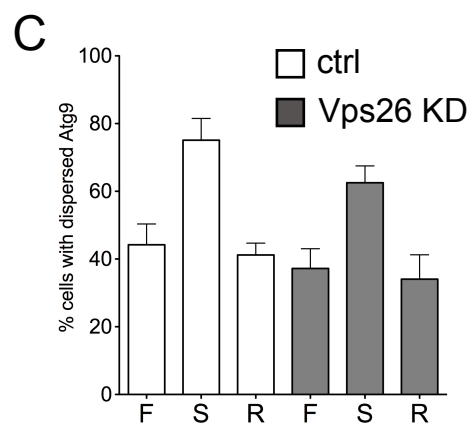
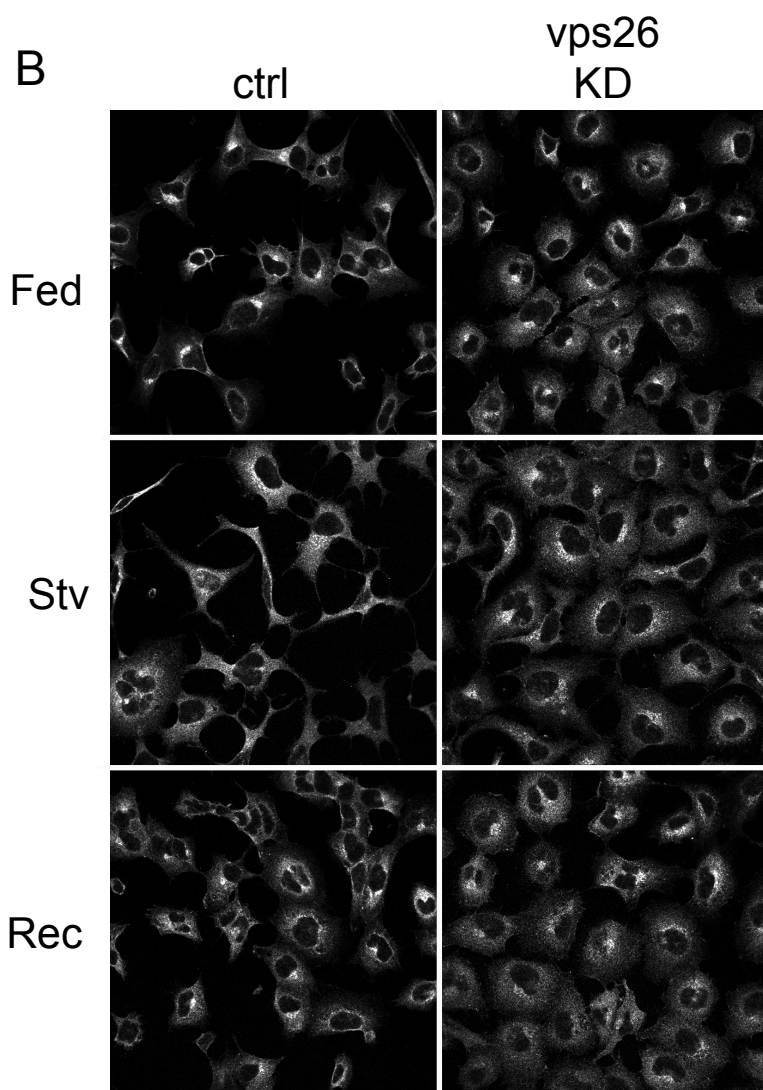
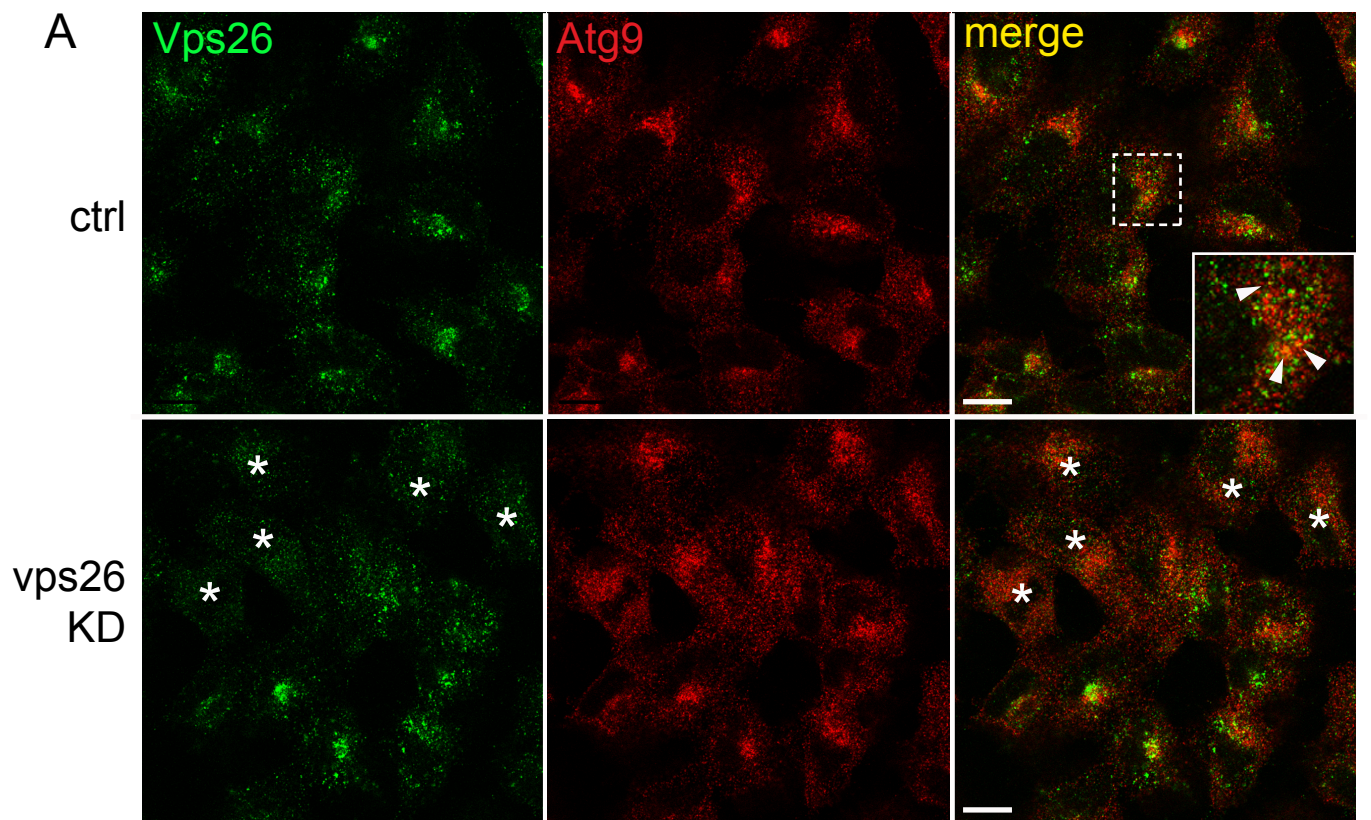


Fig. S5

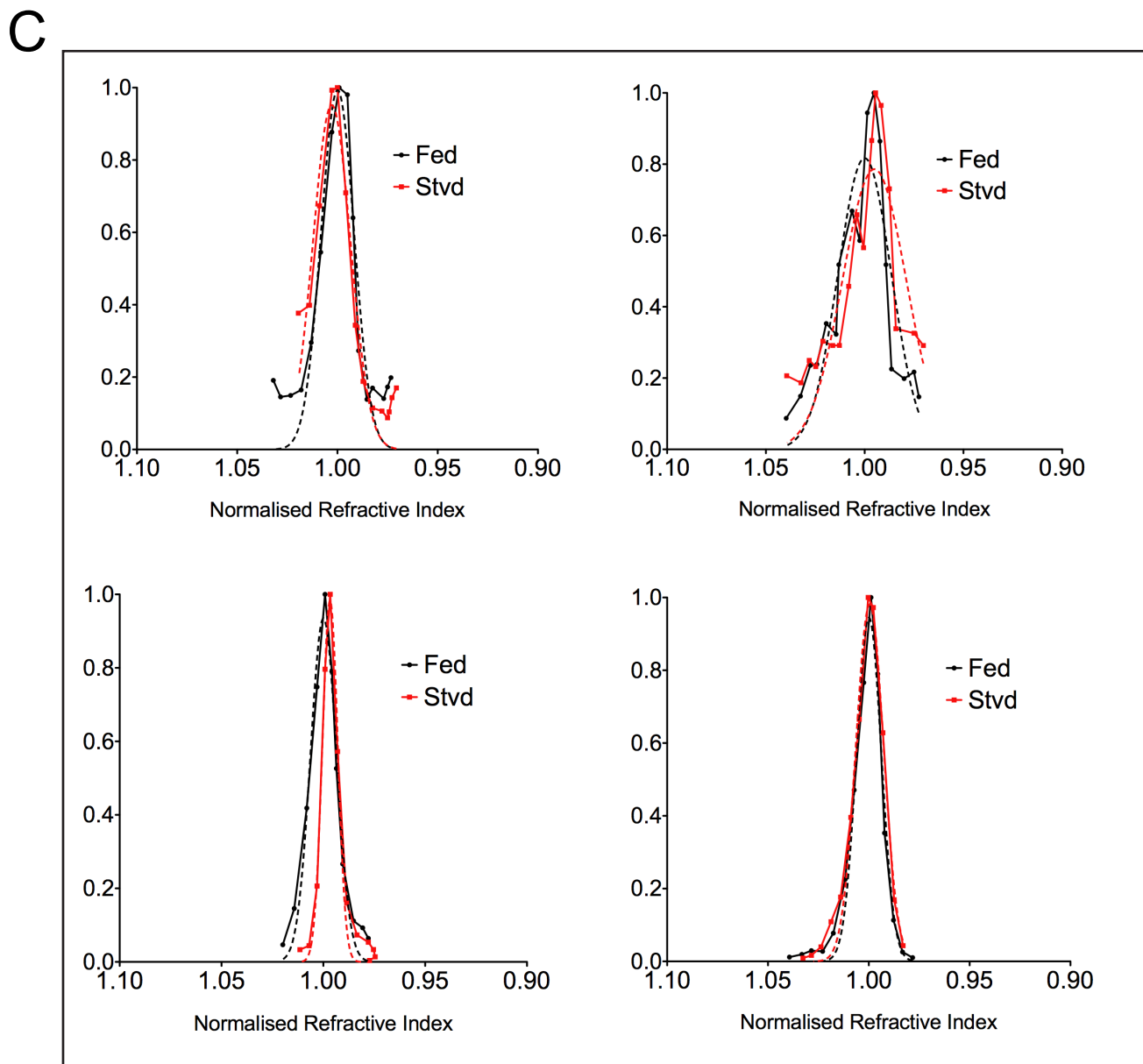
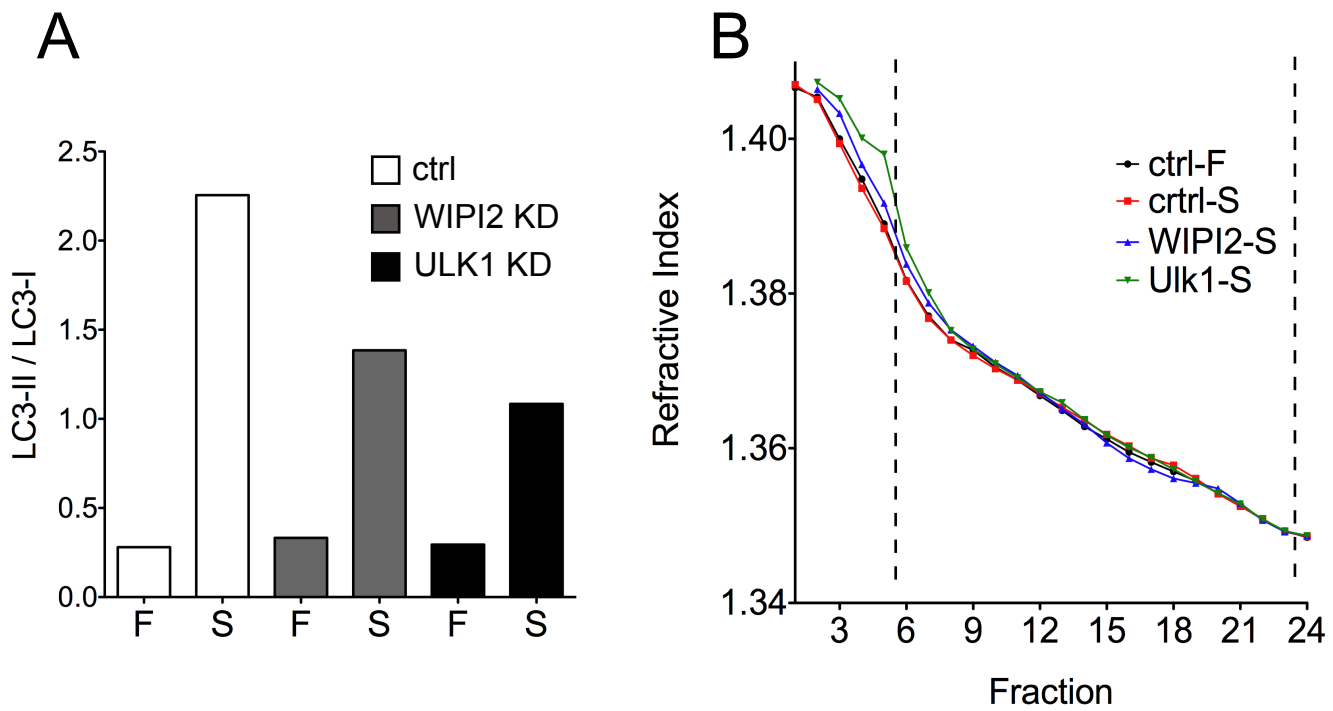


Fig. S6